Improved Algorithm for Fully-automated Neural Spike Sorting based on Projection Pursuit and Gaussian Mixture Model

Kyung Hwan Kim

Abstract: For the analysis of multiunit extracellular neural signals as multiple spike trains, neural spike sorting is essential. Existing algorithms for the spike sorting have been unsatisfactory when the signal-to-noise ratio (SNR) is low, especially for implementation of fully-automated systems. We present a novel method that shows satisfactory performance even under low SNR, and compare its performance with a recent method based on principal component analysis (PCA) and fuzzy c-means (FCM) clustering algorithm. Our system consists of a spike detector that shows high performance under low SNR, a feature extractor that utilizes projection pursuit based on negentropy maximization, and an unsupervised classifier based on Gaussian mixture model. It is shown that the proposed feature extractor gives better performance compared to the PCA, and the proposed combination of spike detector, feature extraction, and unsupervised classification yields much better performance than the PCA-FCM, in that the realization of fully-automated unsupervised spike sorting becomes more feasible.

Keywords: Gaussian mixture model, neural spike sorting, projection pursuit, unsupervised classification.

1. INTRODUCTION

The extracellular recordings of action potentials from multiple neurons have been a major means for the investigation of the nervous system [1,2], and recently they are also being exploited as a major tool for the brain-machine interface [3,4]. A single electrode site gives action potentials from several neurons that are close to the electrode site under investigation, thus it is necessary to transform the recorded waveform into spike trains from each neuron. This procedure is called neural spike sorting. Many automatic and semi-automatic spike sorting methods have been proposed during the past several decades [5,6].

Fig. 1(a) presents a detailed illustration of neural spike sorting procedure. From a microelectrode placed in extracellular space, action potentials from many single neurons adjacent to the electrode site, which are called 'units', are acquired. Since the information of the nervous system is mainly encoded in the timing or occurrence rates of action potentials from single neurons, the multiunit extracellular recording should be separated into multiple spike trains in which the timing of each action potential firing can be determined. As shown in Fig. 1(b), the spike sorting system is usually composed of a dimensionality reduction stage, and a pattern classifier. The input and output of the system is the detected action potential waveform and the label of each waveform, i.e., the name of neuron to which the input waveform belongs. Each detected action potential waveform yields a feature vector, and the dimension is reduced so that it can be effectively handled by an unsupervised classifier. The number of units must also be estimated from the data, without prior knowledge.

Under the condition when a supervised classifier can be used, acceptable results can be obtained even under very high background noise as shown in [7] and [8]. However, a fully-automated method for the spike sorting is necessary, at least in the first analysis of experimental data, which sets a basis for the further analysis where the supervised classification algorithm is used for the spike sorting. Zouridakis and Tam [9] suggested a method to solve this problem, regarding this as a template identification problem. Although this is correct when the template matching is used for the supervised sorting, it is not so when a more powerful algorithm is used for the supervised classification. For example, when Mahalanobis distance is used as a criterion for the spike sorting, the distribution of feature vectors within each cluster as well as the template waveform of each cluster must be known. When a neural-network-type classifier such as

Manuscript received July 29, 2005; revised June 13, 2006; accepted July 19, 2006. Recommended by Editorial Board member Hoon Kang under the direction of Editor Jin Young Choi. The author was supported by a grant from the Korea Health 21 R&D Project, Ministry of Health & Welfare, Republic of Korea (Grant number: A050251).

Kyung Hwan Kim is with the Department of Biomedical Engineering, Yonsei University, 234, Maeji, Heungup, Wonju, Kangwon 135-703, Korea (e-mail: khkim0604@yonsei.ac.kr).

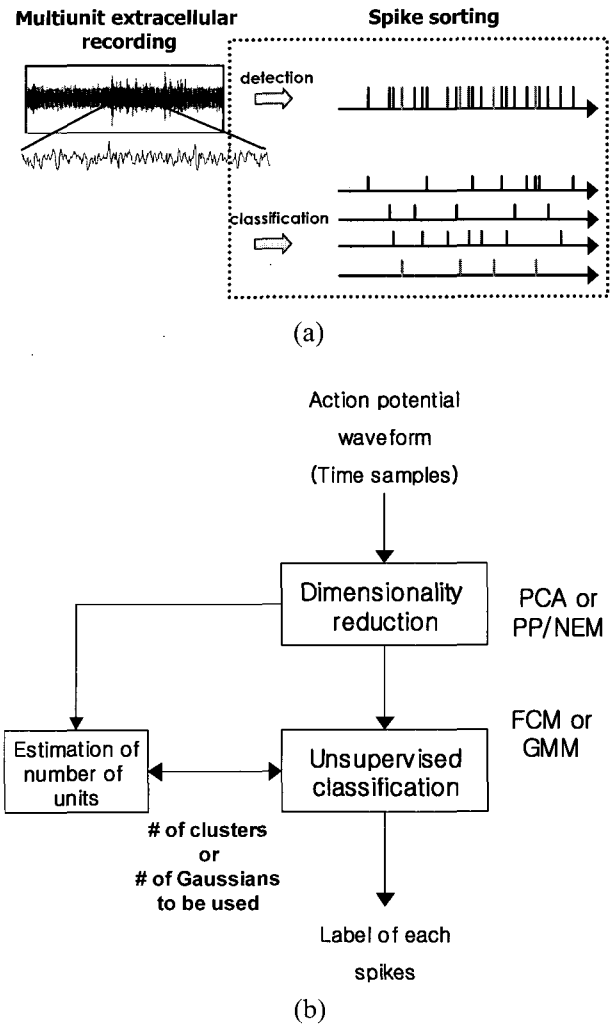

Fig. 1. (a) Illustration of neural spike sorting procedure. (b) Block diagram of the fully-automated neural spike sorting system.

multilayer perceptron or support vector machine is used, the true class label of each feature vector in the training set should be known. This clarifies the necessity of the full procedure of unsupervised classification for the fully-automated spike sorting.

In several recent studies including Fee *et al.* [10], Sahani [11], and Shoham *et al.* [12], the performances under low signal-to-noise ratio (SNR) conditions have not been demonstrated. Recently, we also have proposed a novel unsupervised spike sorting algorithm and have shown its high performance under low SNR [13]. Our approach was to combine projection pursuit based on negentropy maximization (PP/NEM), and an unsupervised classification algorithm based on the modeling of probability density function (pdf) by Gaussian mixture model (GMM). We also proposed an efficient spike detector that shows high performance under low SNR using wavelet transform [14].

In this paper we present a system for fully-automated spike sorting by combining those two previous results, and give a more detailed presentation of the superior performance of our method in implementing the fully automated spike sorting. We also provide a comparison between our method and an unsupervised spike sorting based on principal component analysis (PCA), and fuzzy c-means (FCM) clustering [15]. Although it is a natural choice for the projection, the performance of the PCA as a feature extractor for spike sorting is not satisfactory under low SNR, and even when the SNR is quite high, the PCA may give unsatisfactory results as we demonstrate in this paper.

Although the k-means-type clustering algorithms have been applied for many problems involving unsupervised pattern classification and suggested as a method to implement a fully automated spike sorting [15,16], it may yield insufficient performance, since the shape of distribution of feature vectors cannot be considered. In addition, cluster validity indices, which were proposed to estimate the number of clusters for the k-means-type clustering algorithms [17], does not give robust estimation of the true number of units in the detected action potential waveforms. Our methods can take into account the anisotropic shape of distribution, and thus provide a solution to the problem of determining the number of units in the recording.

2. SPIKE DETECTION AND SORTING ALGORITHM

Fig. 1(b) shows the overall structure of our spike sorting system. Detected action potential waveforms are given to the block that performs dimensionality reduction, after which extracted feature vectors are given as input to the unsupervised classifier. Dimensionality reduction is employed because successful training of the unsupervised classifier became much easier after the dimensionality reduction. Here we suggest a novel method using PP/NEM for the feature extraction, and GMM for the unsupervised classification.

2.1. Wavelet-transform-based spike detector

Typically, a wavelet basis has a spiky waveform shape. The scale (i.e., the time duration) of the basis is varied during the procedure of wavelet transform. Thus at some particular scales where the duration of neural spikes and that of the scaled wavelet basis are matched, the wavelet basis provides a useful approximation to the matched filter, which is known to be the optimal linear filter for the waveform detection. If the match between the neural spike waveform and the scaled basis is perfect, and the background noise is white Gaussian, the wavelet basis can be regarded as the matched filter. In this regard,

although this assumption is not valid obviously in practice, an efficient detector can be devised, by performing wavelet decomposition over many scales and selecting some of the scales which are matched to the duration of the action potential waveform.

The details of the procedure are described below. First, the absolute values of wavelet coefficients are calculated for 5 dyadic scales, i.e., 2^1~2^5. The scale where the absolute value yields a maximum, called, is selected. Subsequently, the point-wise product of the wavelet coefficients over three successive scales up to $2^{j\max}$, $P(n)$, is calculated for all time samples, n, as follows:

$$P(n) = \prod_{j=j_{\max}-2}^{j_{\max}} \left| W(2^j, n) \right|. \quad (1)$$

We found that the choice of three consecutive dyadic scales up to $2^{j\max}$ is appropriate for most cases of neural spike detection. The inclusion of very large or small scales considerably decreased the signal peaks in the waveform of $P(n)$ because correlation between the scaled wavelet basis and the target signal (neural spike) is decreased for those scales. When too coarse a scale is included, the signal peaks in $P(n)$ also decreased because of a large mismatch in the location of peaks among different scales. The wavelet decomposition into dyadic scales is computed by discrete wavelet transform (DWT). The DWT can be performed by successive applications of a bank of quadrature mirror filters and decimation by factor of two between them. The coiflet basis function was adopted.

Finally the $P(n)$ is smoothed by convolution with the Bartlett window to lessen malicious effects of spurious peaks due to cross terms, background noise, and mismatches in the location of the signal peaks among different scales. The window length was empirically determined to be about half the duration of the neural spike. The final output of the proposed action potential detector, $T(n)$, is expressed as follows:

$$T(n) = w(n) * P(n) = w(n) * \left(\prod_{j=j_{\max}-2}^{j_{\max}} \left| W(2^j, n) \right| \right). \quad (2)$$

Here $w(n)$ denotes the Bartlett window.

2.2. Feature extraction and automated unsupervised classification

A dimensionality reduction based on linear transform is used for the feature extraction. The linear transform is expressed as $\mathbf{y}=\mathbf{W}^T\mathbf{x}$ where $\mathbf{x}$ is m-dimensional observed vector (in this case, samples of the detected action potential waveform), $\mathbf{y}$ is n-dimensional random vector ($n \le m$), and $\mathbf{W}$ is an $m \times n$ matrix. The projection matrix $\mathbf{W}$ must be determined so that the components of $\mathbf{y}$ become discriminative features, that is, the separability among clusters is maximized. This type of problem is called projection pursuit (PP). The PCA is also a kind of linear transform, but the transformation matrix for the PCA is obtained by a criterion of maximal variance. Although it can be regarded as an optimal linear projection for the data representation, it is not so for the pattern classification. An appropriate objective function must be defined to find W that maximizes the separability for the projection pursuit. The measure of non-Gaussianity is appropriate for this purpose considering the well-known fact that the multimodality of given high dimensional data might be represented most lucidly in the direction where non-Gaussianity is maximized [18], and the multimodality in the resulting distribution is desirable for clustering [19]. It is also well known that entropy is minimized for the most non-Gaussian distribution; since it has a small value for the distribution that is concentrated on certain values, i.e., when the variable is clearly clustered. This relation of non-Gaussianity and entropy is used to derive the projection that maximizes separability. We call the employed method of dimensionality reduction projection pursuit based on negentropy maximization (PP/NEM). The detailed procedure of performing PP/NEM is described in [13].

In many cases where the feature extraction is performed by a linear transform, the extracted feature vectors form a distribution with elongated shape because the degree of scatter is different for each component. Therefore we can deduce that an unsupervised classification method, by which the cluster shape can be considered, should yield much improved performance. In the case where the FCM is used for the classification, cluster validity index is used for the determination of the number of clusters. The cluster validity index is defined as a ratio of the spread within a cluster and the distance among each cluster's centroids. By calculating the index as a function of the tentative number of clusters, it is possible to estimate the true number of clusters since we can assume that the true number of clusters corresponds to the one that yields minimum index. It is because the index is minimized when the spread within a cluster is minimized and the distance among cluster centroids is maximized. The details on FCM and cluster validity index, and their application to the fully automated spike sorting are given in Xie and Beni [17] and [15], respectively.

The GMM-based clustering has been utilized for many unsupervised pattern classification problems [20]. It was also used for the neural spike sorting by Sahani [11]. We focused on the problem of determining the optimal number of Gaussians in the mixture for the spike sorting. We showed that this problem can be settled by using a roughly estimated

number of Gaussians and then subsequently seeking the modes of the obtained pdf model.

The GMM model is defined as follows:

$$p(\mathbf{x}) = \sum_{m=1}^{K} p(m)p(\mathbf{x} \mid m) = \sum_{m=1}^{K} \pi_m p(\mathbf{x} \mid m). \quad (3)$$

Here π_m is the prior probability of the m'th Gaussian. K denotes the number of Gaussians used to represent the pdf of given data. Each $p(\mathbf{x}|m)$ is a Gaussian distribution function, i.e.,

$$p(\mathbf{x} \mid m) = g(\mathbf{x} \mid \boldsymbol{\mu}_m, \boldsymbol{\Sigma}_m) = g(\mathbf{x} \mid \boldsymbol{\theta}_m) \quad (4)$$
$$= \left|2\pi\boldsymbol{\Sigma}_m\right|^{-\frac{1}{2}} \exp\left(-\frac{1}{2}(\mathbf{x}-\boldsymbol{\mu}_m)^T \boldsymbol{\Sigma}_m^{-1}(\mathbf{x}-\boldsymbol{\mu}_m)\right).$$

Here $g(\mathbf{x}|\mu_m,\Sigma_m)$ is the m'th Gaussian whose mean vector and covariance matrix are μ_m, and Σ_m respectively. The parameter vectors of GMM, θ can be iteratively estimated by the application of expectation-maximization (EM) algorithm [20].

The number of Gaussians in GMM, K, must be determined prior to the parameter estimation. Although it is expected that a considerable amount of variability in the resulting GMM pdf model might occur when different K values are used, the obtained pdf models are quite similar for different K's in the case of neural spike sorting if K value is slightly larger that the actual number of clusters. In this case, when the means of two specific Gaussians are close to each other, these two are merged to form a single peak and the number of modes of overall estimated pdf becomes the same as the number of units in the recording.

The problem of determining K for the GMM parameter estimation can be considered to be a decision problem where the maximum-(log) likelihood (ML) estimation can be applied. However, the likelihood is a monotonically increasing function of the number of parameters; a number of criteria for the determination of the number of parameters, such as Akaike's information criteria (AIC) have been proposed [21]. However, they often fail to give a satisfactory result in practice. Instead, we use a method based on the behavior of the log-likelihood vs. K curve. This curve typically shows rapid initial increment behavior, followed by a slow increment [22]. The actual number of clusters is located slightly above the 'knee' of this curve. A satisfactory estimation of the GMM parameters is possible when the value of K is set to be slightly larger than the actual number of clusters and does not need to be accurate; it is possible to determine the value of K to be used as follows. First, the log-likelihood is calculated for several values of the number of Gaussians and then, the position of the 'knee' is determined by finding the maximum of the derivative of the log-likelihood with respect to the number of Gaussians.

An actual procedure for applying the identified GMM to the unsupervised neural spike sorting is as follows. Because the number of Gaussians can be different from the true number of units, in order to use the obtained GMM for classification, it is necessary to identify the number and position of 'modes' (local maxima of GMM) in the mixture model of pdf, and to assign each Gaussian in the mixture to a specific mode. After identifying the local maxima, each mean of Gaussians is assigned to the closest local maximum so that the pdf of a single cluster (i.e., a single unit) can be represented by a partial sum of the Gaussians as follows:

$$p_l(\mathbf{x}) = \sum_{m=1}^{L} \pi_m g(\mathbf{x} \mid \boldsymbol{\mu}_m, \boldsymbol{\Sigma}_m), \quad (5)$$

where $p_l(\mathbf{x})$ denotes the pdf of the l'th cluster, and L is the total number of Gaussians, the center of which is closest to the l'th mode. The class label of a particular data point $\mathbf{x}$ is determined from the label of maximum pdf. The mode-finding of the GMM is performed by quadratic maximization or gradient ascent method [23]. This procedure is facilitated by the closed-form expression of the gradient and Hessian of the GMM [24].

3. EXPERIEMENTS

The details of the extracellular neural signal recording have been described thoroughly in Kim and Kim [8], and Yoon *et al.* [25]. The extracellular recordings from the somatosensory cortex of a Sprague-Dawley rat and the abdominal ganglion of the Aplysia were performed using thin-film semiconductor microelectrodes, the impedance ranges of which were 2-3 MΩ at 1 kHz. Bandpass filtering (100 Hz – 5 kHz for the Aplysia recording, 300 Hz – 3 kHz for rat recording, respectively) was employed. The sampling rate was 10 ksamples/sec and 20 ksamples/sec, for the Aplysia and rat recording, respectively. The template waveforms were extracted by a human supervisor assisted by efficient neural spike detectors described in [8] and Kim and Kim [14], and the FCM clustering of waveforms at a reasonably high SNR. The action potential segments consisted of 25 samples and 40 samples for the Aplysia and for the rat recording, respectively. The template waveforms of the action potentials from three single neurons extracted from the rat recording are shown in Fig. 2, and those of the Aplysia recording can be found in [8].

We also obtained the autoregressive (AR) models of background noise from the neural signal recordings, in order to generate test data that faithfully represents

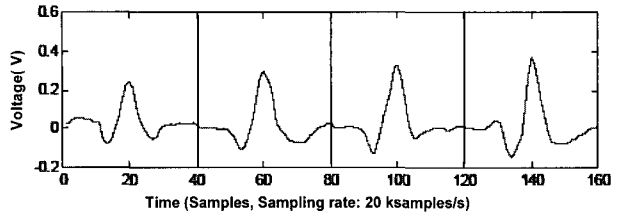

Fig. 2. Four template waveforms of the action potentials from rat somatosensory cortex. Each unit consists of 40 samples (2 ms).

the actual characteristics of experimental recordings. The AR model coefficients were identified from background noise segments of approximately 300 samples by Burg's algorithm [26] along with order determination using Akaike information criteria. Accurate determination of the order was not essential for effective modeling. From the template waveforms of several units and the AR model of the background noise, it becomes possible to generate the waveforms of arbitrary SNR that have the characteristics of real experimental recordings.

4. RESULTS

4.1. Comparison of PCA and PP/NEM for feature extraction in spike sorting system

For the purpose of quantitative comparison of the efficacies of linear transforms, we used two performance indices based on scatter matrix. Each index is a function of transform matrix **W**. The first index is used for Fisher's linear discriminant analysis, and is defined as follows:

$$J_1(\mathbf{W}) = \frac{\det(\tilde{\mathbf{S}}_B)}{\det(\tilde{\mathbf{S}}_W)} = \frac{\det(\mathbf{W}^T\mathbf{S}_B\mathbf{W})}{\det(\mathbf{W}^T\mathbf{S}_w\mathbf{W})}, \tag{6}$$

$$\mathbf{S}_w = \sum_{i=1}^{c}\mathbf{S}_i, \quad \mathbf{S}_i = \sum(\mathbf{x}-\mathbf{m}_i)(\mathbf{x}-\mathbf{m}_i)^T, \tag{7}$$

$$\mathbf{S}_B = \sum_{i=1}^{c}(\mathbf{m}_i-\mathbf{m})(\mathbf{m}_i-\mathbf{m})^T,$$

where $\mathbf{x}$, $\mathbf{m}_i$, and $\mathbf{m}$ means the feature vector, the mean vector of the ith cluster, and the overall mean vector, respectively.

Because the determinant of the scatter matrix corresponds to the square of the volume of hyper-ellipsoidal scattering, $J_1(\mathbf{W})$ is the ratio between the separation of each cluster and the scattering within a single cluster. The second index, which can be interpreted in similar context, is defined as follows:

$$J_2(\mathbf{W}) = Trace((\mathbf{W}^T\mathbf{S}_w\mathbf{W})^{-1}\mathbf{W}^T\mathbf{S}_B\mathbf{W}). \tag{9}$$

Fig. 3(a) and (b) show the separability indices

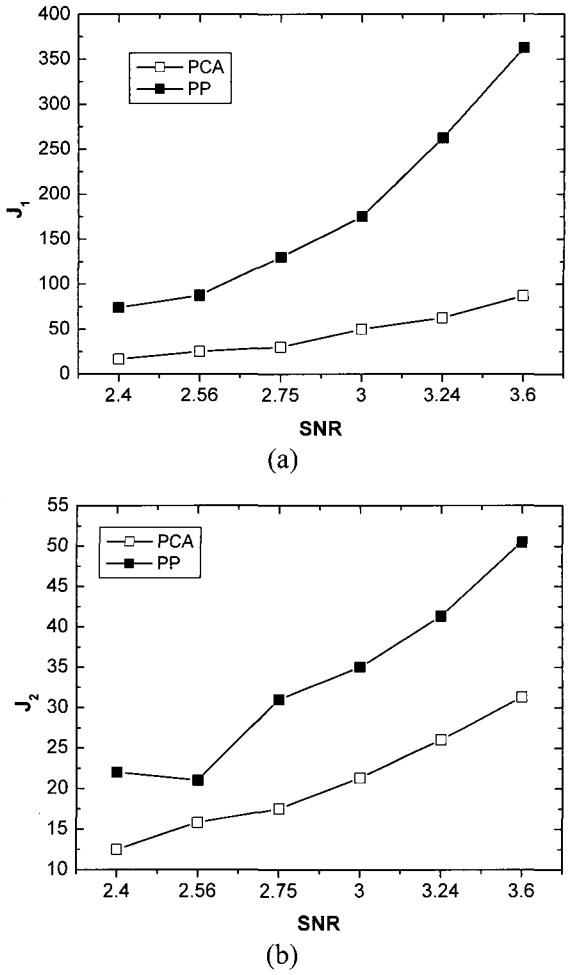

Fig. 3. Separability indices (a) J_1 and (b) J_2 obtained for the four unit rat cortex data under various SNRs.

under various SNRs (three unit rat cortex data). It is shown that the PP/NEM is superior to the PCA for a broad range of SNRs. The separability indices were obtained from the data where 2100 waveforms (700 waveforms for each unit) were included. For some data where one of the units has a template waveform distinctly different from the other two (shown in Fig. 4(a)), the PCA gave better separability as indicated by the scatter plot in Fig. 4(b) and (c). However, considering the discrimination of similar waveforms, the PP/NEM demonstrated better performance also as shown in Fig. 5. Fig. 5(b) and (c) present the results of projection by the PP/NEM and PCA when another unit with a waveform similar to the two waveforms in Fig. 4(a) is added (see Fig. 5(a)). The PCA results in a severe overlap among clusters of similar template waveforms, whereas the PP/NEM consistently gives reasonable projections. The PP/NEM consistently showed superior performance, thus justifying our choice of the PP/NEM for the fully-automated spike sorting. We also compared the efficacies of PP/NEM and PCA, for the classification. Fig. 6(a) and (b) show

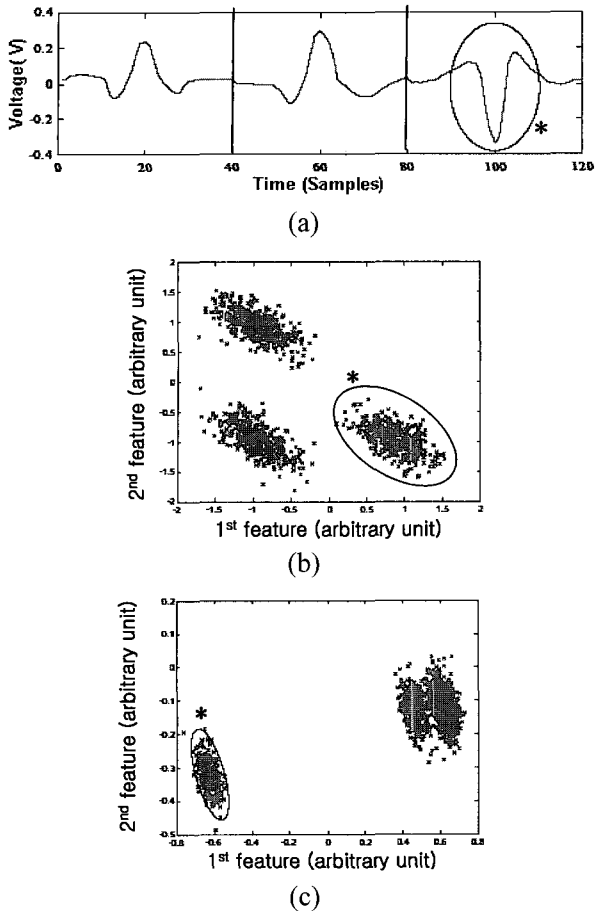

Fig. 4. Projection of the rat cortex data where one of the units (denoted by '*') has template waveform distinctly different to the other two. (a) Template waveforms; (b) PP/NEM scatter plot; (c) PCA scatter plot. Here, the PCA gives better separability.

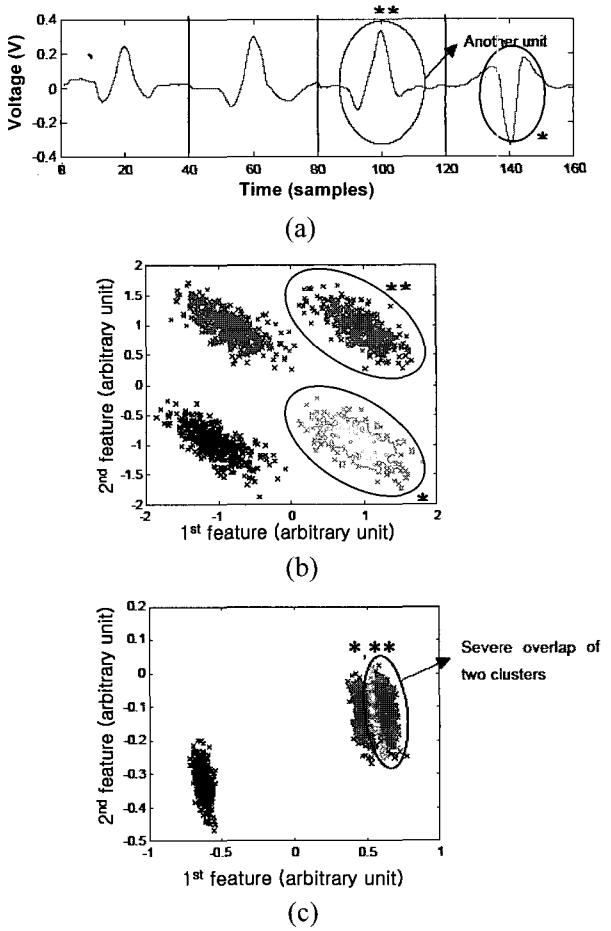

Fig. 5. Projection by the PP/NEM and PCA when another unit with waveform similar to the two waveforms in Fig. 4 (denoted by '**') is added. PCA results in a severe overlap among clusters of similar template waveforms, whereas the PP/NEM consistently gives reasonable projections. (a) Template waveforms; (b) PP/NEM scatter plot; (c) PCA scatter plot.

clustering results by gray level when the PCA and PP/NEM were used for feature extraction, respectively. It became obvious that successful unsupervised sorting is possible by using FCM after PP/NEM, for the data where the FCM is inapplicable after the PCA.

However, in some cases when the extracted feature vectors formed an elongated cluster shape and when inter-cluster distances were short (for example, Fig. 7(a)), the FCM often yielded a totally incorrect clustering result as seen in Fig. 7(b), because the distances between data points and the means were represented by Euclidean distance so that cluster shape cannot be considered for clustering. In this case, the determination of the number of units by the cluster validity index was not possible, either. This clarifies the necessity of an unsupervised classification method by which non-spherical (anisotropic) cluster shape can be considered.

4.2. Performance of the PP/NEM-GMM spike sorting algorithm

We demonstrate the performance of the PP/NEM-GMM spike sorting system for the data where a successful clustering was impossible by the PP/NEM-FCM as in the case of Fig. 7(b). Fig. 7(c) shows the estimated pdf using four Gaussians. It is clear that we could obtain quite a reasonable result having three peaks. Next, Fig. 7(d) shows the result of pdf estimation using five Gaussians. The use of five Gaussians also yielded reasonable results, and thus, it was demonstrated that the result of pdf modeling by the GMM was not dependent so much on the number of Gaussians. Therefore the classification result should be much less affected by a parameter that must be predetermined compared to the case of k-means-type algorithms, so that the fully-automated system based on the GMM would be expected to be much more reliable.

The estimation of the modes (local maxima) of the

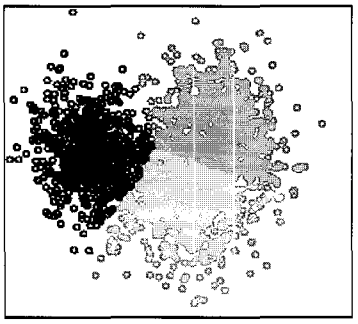

(a)

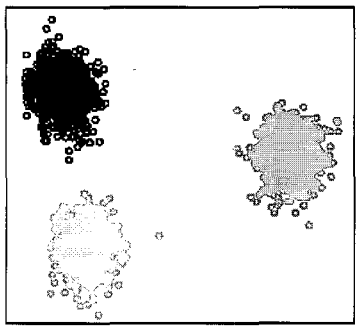

(b)

Fig. 6. Efficacy of each projection methods on clustering. (a) On the projected data using PCA. (b) On the projected data using PP/NEM.

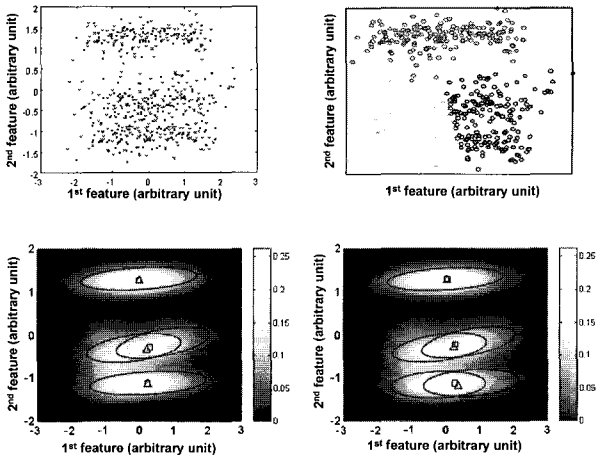

Fig. 7. Application of the proposed projection and GMM pdf model identification for an *Aplysia* recording with SNR≈1.25. Upper left: Projection result using PP/NEM Upper right: Clustering result using the FCM algorithm (different clusters appear in varying shades of gray scales). Lower left: GMM pdf model using four Gaussians. Lower right: GMM pdf model using five Gaussians.

GMMs, which correspond to the average waveforms of each unit, was successful for the two cases (using 4 and 5 Gaussians). The modes found are shown as

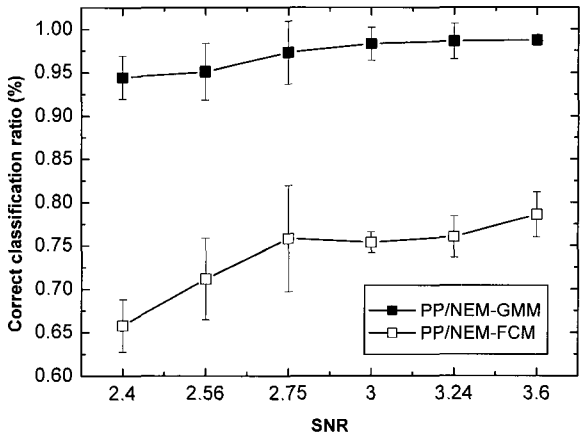

Fig. 8. Performances of PP/NEM-GMM and PP /NEM-FCM spike sorting systems. Correct classification ratio under various SNRs were calculated (ten rat somatosensory cortex recordings with 2100 neural spikes were tested for each SNR).

triangles, and the locations of the projections of the true template waveforms are denoted by squares in Fig. 7(c) and (d). The classification success rates were virtually the same for two cases (96.5 and 96.2% for 4 and 5 Gaussians, respectively). When we used PP/NEM-FCM with the proper number of clusters (3 clusters), the best success rate obtained was only 67 %.

We compared the performances of PP/NEM-FCM and PP/NEM-GMM sorting systems in detail under various SNR's. Fig. 8 demonstrates the advantage of our method clearly. Correct classification ratios were shown as a function of SNR. For each SNR, ten recordings with 2100 neural spikes (700 for each unit) were given as input to the spike sorting system. The dimension of projected feature vectors were fixed to two, since the increase of dimension gave no considerable performance improvement and was computationally inefficient (mainly due to the computational burden in GMM parameter estimation using EM algorithm).

5. DISCUSSION AND CONCLUSIONS

The fully automated spike sorting is essential in the first analysis of multiunit extracellular neural signal. The importance of this system has been pointed out in several recent studies [27,28], however, a detailed presentation of the sorting performance under low SNR has not been reported. The purpose of this paper was to give a comprehensive presentation of the superior performance of the fully automated spike sorting system based on the combination of PP/NEM-GMM under various situations. By applying a feature extraction/dimensionality reduction using negentropy maximization, we could achieve much higher separability than conventional methods such as PCA.

The problem of anisotropic cluster shape and close distance of each cluster prevented successful unsupervised classification using the clustering algorithms based on Euclidean distance, such as the *k*-means algorithm. The problem was alleviated by modeling overall distribution of feature vectors as the GMM. After that, local maxima of the GMM were sought, and each mean of Gaussians in the mixture was assigned to one of these local maxima. In order to deal with a severely non-Gaussian background noise, an unsupervised classification using mixture of *t*-distribution [12] may be employed while retaining the structure of the proposed spike sorting algorithm.

It was shown that its performance is better than the PCA-FCM system in two respects: 1) superiority under low SNR, 2) superiority for the fully-automated system (i.e., it is not so much dependent on the parameter that should be predetermined.). In the past, manual analysis by the human supervisor was a good choice, because it showed often better performance than many automatic algorithms and only a few channels were analyzed (although it is tedious). However, for the purpose of multichannel recording up to hundreds of channels [27], the importance of capability of the fully automated system is evident. Because of the advance of multichannel electrodes and the computational hardware, the automated detection and classification system will become indispensable in the future as an essential preprocessing stage for the further study of neuronal systems involving analysis of the multiple neuronal spike train. It will be possible to find many applications of the fully automated spike sorting system, in that it is becoming more important to investigate the interrelated behavior of the network of neurons by analyzing hundreds of channels of neural signal recording.

Whereas it has been conventional to analyze the recordings showing sufficiently good quality, it is greatly beneficial if the range of signal quality that can be analyzed becomes much broader. Especially, for the long-term recording whose signal quality can be degraded in an unpredictable way, successful operation of the fully automated spike sorting under high background noise provides a significant advantage [28].

The proposed method of estimating the overall distribution as a mixture of Gaussians, and subsequent classification can be applied without loss of generality to the cases where the distribution within a single class is considerably different from Gaussian. In this case, each sub-pdfs can be modeled as a non-Gaussian distribution function, such as *t*-distribution [12].

REFERENCES

[1] R E. N. Brown, L. M. Frank, D. Tang, M. C. Quirk, and M. A. Wilson, "A statistical paradigm for neural spike train decoding applied to position prediction from ensemble firing patterns of rat hippocampal place cells," *J. Neurosci.*, vol. 18, pp. 7411-7425, 1998.

[2] D. K. Warland, P. Reinagel, and M. Meister, "Decoding visual information from a population of retinal ganglion cells," *J. Neurophysiol.*, vol. 78, pp. 2336-2350, 1997.

[3] J. Wessberg, C. R. Stambaugh, J. D. Kralik, P. D. Beck, M. Laubach, J. K. Chapin, J. Kim, S. J. Biggs, M. A. Srinivasan, and M. A. L. Nicolelis, "Real-time prediction of hand trajectory by ensembles of cortical neurons in primates," *Nature*, vol. 408, pp. 361-365, 2000.

[4] K. V. Shenoy, D. Meeker, S. Cao, S. A. Kureshi, B. Pesaran, C. A. Buneo, A. P. Batista, P. P. Mitra, J. W. Burdick, and R. A. Andersen, "Neural prosthetic control signals from plan activity," *NeuroReport*, vol. 14, pp. 1-6, 2003.

[5] E. M. Schmidt, "Computer separation of multi-unit neuroelectric data: A review," *J. Neurosci. Meth.*, vol. 12, pp. 95-111, 1984.

[6] M. S. Lewicki, "A review of methods for spike sorting: the detection and classification of neural action potentials," *Network: Computa-tion in Neural System*, vol. 9, pp. R53-R78, 1998.

[7] R. Chandra and L. M. Optican, "Detection, classification, and superposition resolution of action potentials in multiunit single channel recordings by an on-line real-time neural network," *IEEE Trans. Biomed. Eng.*, vol. 44, pp. 403-412, 1997.

[8] K. H. Kim and S. J. Kim, "Neural spike sorting under Nearly 0 dB signal-to-noise ratio using nonlinear energy operator and artificial neural network classifier," *IEEE Trans. Biomed. Eng.*, vol. 47, pp. 1406-1411, 2000.

[9] G. Zouridakis and D. C. Tam, "Identification of reliable spike templates in multi-unit extracellular recordings using fuzzy clustering," *Comp. Meth. Prog. in Biomed.*, vol. 61, pp. 91-98, 2000.

[10] M. S. Fee, P. P. Mitra, and D. Kleinfeld, "Automatic sorting of multiple unit neuronal signals in the presence of anisotropic and non-Gaussian variability," *J. Neurosci. Meth.*, vol. 69, pp. 175-188, 1996.

[11] M. Sahani, *Latent Variable Models for Neural Data Analysis*, Ph.D. dissertation, California Institute of Technology, 1999.

[12] S. Shoham, M. R. Fellows, and R. A. Normann, "Robust, automatic spike sorting using mixtures of multivariate *t*-distributions," *J. Neurosci. Meth.*, vol. 127, pp. 111-122, 2003.

[13] K. H. Kim and S. J. Kim, "Method for unsupervised classification of multiunit neural signal recording under low signal-to-noise

ratio," *IEEE Trans. on Biomed. Eng.*, vol. 50, pp. 421-431, 2003.

[14] K. H. Kim and S. J. Kim, "A wavelet-based method for action potential detection from extracellular neural signal recording with low signal-to-noise ratio," *IEEE Trans. on Biomed. Eng.*, vol. 50, pp. 999-1011, 2003.

[15] G. Zouridakis and D. C. Tam, "Identification of reliable spike templates in multi-unit extracellular recordings using fuzzy clustering," *Comp. Meth. Prog. in Biomed.*, vol. 61, pp. 91-98, 2000.

[16] P. Zhang, J. Wu, Y. Zhou, P. Liang, and J. Yuan, "Spike sorting based on automatic template reconstruction with a partial solution to the overlapping problem," *J. Neurosci. Meth.*, vol. 135, pp. 55-65, 2004.

[17] X. L. Xie and G. A. Beni, "A validity measure for fuzzy clustering," *IEEE Trans. Pattern Anal., Intell.*, vol. 13, pp. 841-847, Mach 1991.

[18] A. Hyvarinen, "Fast and robust fixed-point algorithms for independent component analysis," *IEEE Trans. Neural Network*, vol. 10, pp. 626-634, 1999.

[19] P. J. Huber, "Projection pursuit," *Ann. Statisti*, vol. 13, pp. 435-475, 1985.

[20] K. Jain, R. P. W. Duin, and J. Mao, "Statistical pattern recognition: A review," *IEEE Trans. Pattern Anal. Mach. Intel.*, vol. 22, pp. 4-37, 2000.

[21] M. Windham and A. Cutler, "Information ratios for validating mixture analysis," *J. Amer. Stat. Assoc.*, vol. 87, pp. 1188-1192, 1992.

[22] D. A. Langan, J. W. Modestino, and J. Zhang, "Cluster validation for unsupervised stochastic model-based image segmentation," *IEEE Trans. Imag. Proc.*, vol. 7, pp. 404-420, 1998.

[23] D. G. Ruenberger, *Optimization by Vector Space Methods*, John Wiley & Sons, 1969.

[24] M. A. Carreira-Perpinan, "Mode-finding for mixtures of Gaussian distribution," *IEEE Trans. Pattern Anal. Mach. Intell*, vol. 22, pp. 1318-1323, 2000.

[25] T. H. Yoon, E. J. Hwang, D. Y. Shin, S. I. Park, S. J. Oh, S. C. Jung, H. C. Shin, and S. J. Kim, "A micromachined silicon depth probe for multi-channel neural recording," *IEEE Trans. Biomed. Eng.*, vol. 47, pp. 1082-1087, 2000.

[26] M. H. Hayes, *Statistical Digital Signal Processing and Modeling*, Wiley, 1996.

[27] E. N. Brown, R. E. Kass, and P. P. Mitra, "Multiple neural spike train data analysis: State-of-the-art and future challenges," *Nature Neurosci.*, vol. 7, pp. 456-461, 2004.

[28] S. Shoham and S. S. Nagarajan, "The theory of CNS recording", in *Neurprosthetics: Theory and Applications*, K. W. Horch and G. S. Dhillon (editors), World Scientific, New Jersey, 2004.

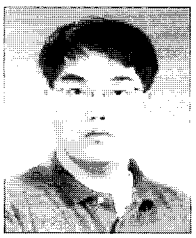

Kyung Hwan Kim received the B.S. degree in Electrical Engineering from the Korea Advanced Institute of Science and Technology (KAIST) in 1995. He received the M.S. and Ph.D. degrees in Electrical Engineering from Seoul National University, Korea, in 1997 and 2001, respectively. From 2001 to 2003, he was a Member of the Research Staff at Samsung Advanced Institute of Technology. In 2003, he also worked as a Visiting Scientist at the fMRI laboratory of the brain science research center at KAIST. Since 2004, he has been with Yonsei University, Wonju, Korea, where he is an Assistant Professor of Biomedical Engineering. His research interests include neural prosthesis, neural signal processing, and multimodal monitoring of the nervous system.